



Low temperature decomposition of NO on ordered alumina films

S. Schauer mann, V. Johánek, M. Laurin, J. Libuda *, H.-J. Freund

Department of Chemical Physics, Fritz-Haber-Institut der Max-Planck-Gesellschaft, Faradayweg 4-6, 14195 Berlin, Germany

Received 1 August 2003; in final form 18 September 2003

Published online: 22 October 2003

Abstract

We have investigated the interaction of NO with an ordered Al₂O₃ film and a Pd/Al₂O₃ supported model catalyst, employing time-resolved IR reflection absorption spectroscopy (TR-IRAS) and molecular beam methods. It is observed that NO undergoes slow decomposition at low sample temperature, resulting in the formation of variety of N_xO_y surface species. The process involves strong structural transformations of the Al₂O₃ film. On Pd/Al₂O₃, decomposition of NO is found to be strongly suppressed. Based on the growth behavior of Pd nucleating at oxide defects, it is concluded that NO decomposition is preferentially initiated at specific defect sites on the alumina.

© 2003 Elsevier B.V. All rights reserved.

1. Introduction

In the case of supported catalysts, it is often found that the reaction mechanisms and kinetics depend on the support. A practical example of a reaction system for which the support plays a pivotal role is the catalytic reduction of NO_x. Recently, this reaction has attracted considerable attention in environmental catalysis due to the fact that modern lean-burn engines produce oxygen-rich exhaust gas conditions, under which conventional three-way catalysts may not operate efficiently [1]. Therefore, alternative reduction pathways and nitrogen storage mechanisms have

been considered. Here, some of the key issues are the mechanism and kinetics of nitrogen surface and bulk compound formation and the decomposition and transport of reactive species between the metal particles and the oxide. Both issues have received little attention from the fundamental point of view, yet.

In the work reported here, we focus on the interaction of NO with the alumina support. For this purpose, we employ a model catalyst, which provides a reduced level of complexity and which can be easily investigated using a variety of surface science techniques. Specifically, we use a well-ordered Al₂O₃ film on NiAl(110), on which Pd nanocrystallites are grown under UHV (ultrahigh vacuum) conditions [2–4]. With the aim of correlating structural information with detailed data on the adsorption behavior and reaction kinetics,

* Corresponding author. Fax: +49-30-84134309.

E-mail address: libuda@fhi-berlin.mpg.de (J. Libuda).

we employ molecular beam techniques combined with in situ IR reflection absorption spectroscopy (IRAS) [5]. In this Letter, we focus exclusively on the interaction of NO with the Al_2O_3 support, both in the presence and absence of supported Pd particles. It is found that NO undergoes a slow and complex decomposition sequence at low temperature, which is critically controlled by the presence of defect sites on the support. The NO adsorption, co-adsorption and dissociation kinetics on the Pd particles themselves will be discussed elsewhere [6–8].

2. Experimental

All experiments were performed in a UHV molecular beam apparatus at the Fritz-Haber-Institute (Berlin) [9]. In this work we utilize an NO beam generated by a doubly differentially pumped effusive source. The NO (Messer Griesheim, >99.5 %) was further purified by cold traps before use. Typical beam intensities around 2.8×10^{14} molecules $\text{cm}^{-2} \text{s}^{-1}$ were employed. Residual gas spectra were recorded with an automated quadrupole mass spectrometer system (ABB Extrel). IR spectra were acquired during NO exposure using a vacuum FT-IR spectrometer (Bruker IFS 66v/S) at a spectral resolution of 2 cm^{-1} .

The alumina film was prepared by sputtering and annealing of a NiAl(1 1 0) single crystal, followed by an oxidation and annealing procedure, the details of which are given elsewhere [10]. Cleanliness and quality of the oxide film were checked via low energy electron diffraction (LEED) and Auger electron spectroscopy (AES). Before the experiment, Pd (>99.9 %) was deposited by evaporation from a rod using a commercial evaporator (Focus, EFM 3) based on electron bombardment (Pd coverage: $2.7 \times 10^{15} \text{ cm}^{-2}$, sample temperature: 300 K). In order to avoid damage by ion bombardment, the sample was biased during Pd evaporation.

3. Results and discussion

Before considering NO adsorption, we briefly summarize some of the previous results on the structure of the $\text{Al}_2\text{O}_3/\text{NiAl}(1\ 1\ 0)$ model support and the growth of the Pd particles, which are essential for this work. More detailed information can be found elsewhere [2,3,10]. The film is well-ordered and atomically flat (see Fig. 1a, from [11]). The most important aspect for the current study is the defect structure of the film, which has been investigated in great detail [2,10]. Here, the most important defects are oxide domain boundaries, which appear as bright lines in

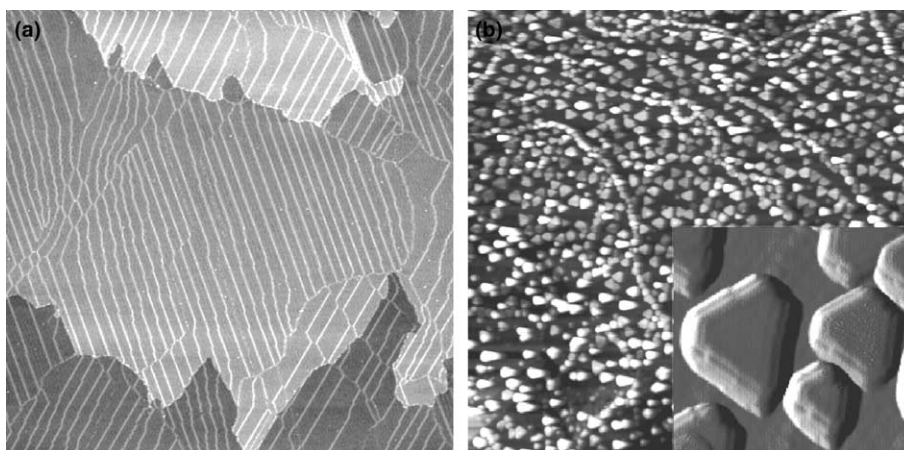


Fig. 1. (a) STM image of the Al_2O_3 film on NiAl(1 1 0) ($500 \text{ nm} \times 500 \text{ nm}$), from [11]. (b) STM image of the Pd particles, grown on the Al_2O_3 film on NiAl(1 1 0) ($300 \text{ nm} \times 300 \text{ nm}$). The inset shows a differentiated close-up ($20 \text{ nm} \times 20 \text{ nm}$), from [3].

Fig. 1a, as well as point defects, which are not resolved in scanning tunneling microscopy (STM) under these conditions.

For the growth of the Pd particles, the oxide defects play a pivotal role, since they tend to act as preferential nucleation centers (see Fig. 1b). The aggregates preferentially nucleate at specific sites at oxide domain boundaries and, consequently, efficiently cover these sites. For the specific system considered in this work, the three-dimensional Pd particles are characterized by an average size of 5.5 nm, contain about 3000 Pd atoms each and exhibit the morphology of well-shaped crystallites, preferentially terminated by (111) facets (see [3] for details).

In the first step we investigate the interaction of NO with the pristine alumina film at a sample

temperature of 100 K. Apparently, the IR spectra (Fig. 2a) show a rather complex behavior: A relatively large exposure of 2×10^{16} molecules cm^{-2} (approximately 60 L; 1 L (Langmuir) = 10^{-6} Torr s corresponds to 3.7×10^{14} NO molecules cm^{-2} at 300 K) is required before first indications of a weak absorption band (3) around 1620 cm^{-1} with a shoulder at lower energy appears. Low energy electron diffraction studies show that the characteristic diffraction pattern of the oxide film vanishes simultaneously (see also [12]). With increasing exposure, the band slowly grows in intensity, before at even higher NO doses around 1×10^{17} molecules cm^{-2} a second band (2) emerges around 1690 cm^{-1} . The latter band grows faster than band (3) and finally dominates the spectrum. After the appearance of band (2) further peaks

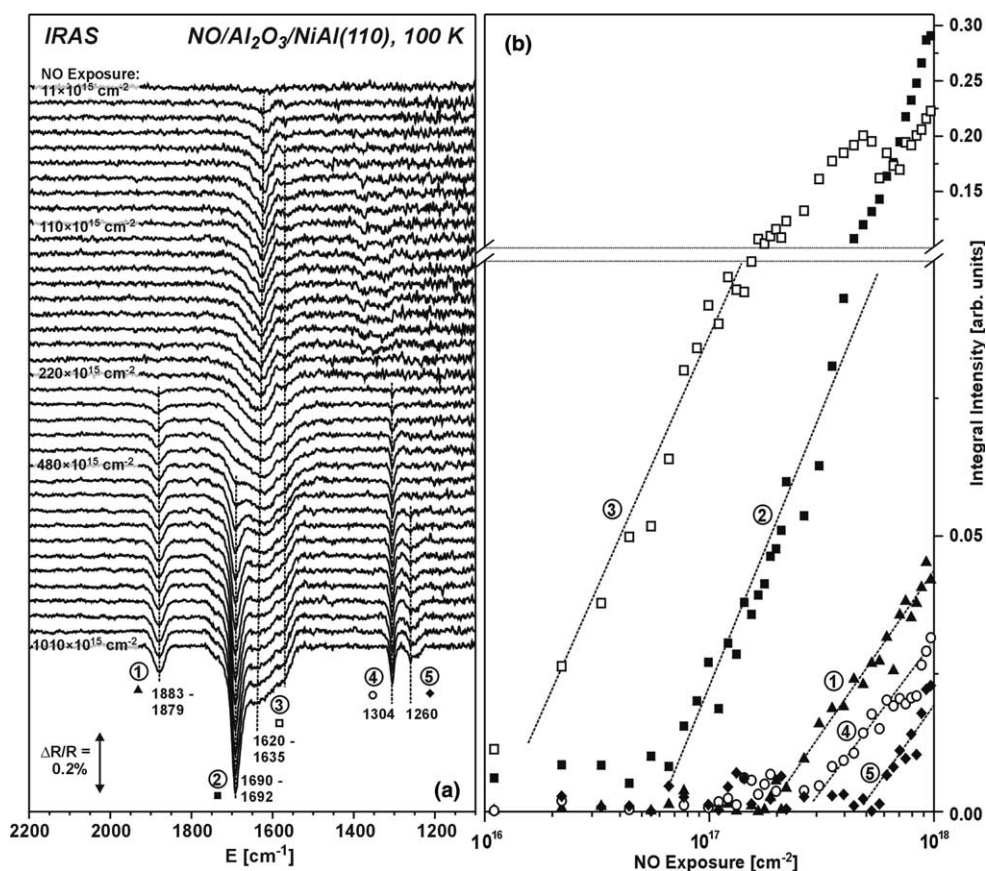


Fig. 2. (a) IR spectra acquired during exposure of the pristine Al₂O₃ film on NiAl(110) to a molecular beam of NO at a sample temperature of 100 K; (b) integral absorption of the different IR bands indicated in (a) as a function of NO exposure.

become visible at 1880 cm^{-1} (1) and 1304 cm^{-1} (4) at NO doses exceeding 2×10^{17} molecules cm^{-2} . Finally, around 5×10^{17} molecules cm^{-2} a weak band at 1260 cm^{-1} (5) appears. The corresponding integral absorption data are displayed in Fig. 2b. Up to the maximal NO dose of 10^{18} molecules cm^{-2} applied, all bands continuously grow in intensity with the exception of band (3) saturating around 3×10^{17} molecules cm^{-2} .

In order to interpret the above data, we consider previous work on the adsorption of NO on different oxide and metal surfaces. Under UHV conditions, NO adsorption on oxidized and bare Mo(110) substrates was studied by Friend and co-workers [13–16]. Moreover, IRAS studies of the behavior of NO on weakly interacting metal surfaces such as Ag(111) [17,18], Cu(111) [19] and Cu(110) [20] as well as on oxide surfaces [21,22] are of relevance for the present case. Under ambient conditions, NO adsorption has been studied on pure alumina [23–25] and on mixed oxides containing alumina [26,27] and the various species observed have been reviewed recently [28].

Monomeric NO species giving rise to absorption features at similar frequency have been observed e.g. on oxygen precovered Mo(110) [14] and on Cu(110) [20]. However, weakly adsorbed NO species on alumina [24,25] and other oxide surfaces [21,22] typically show characteristic absorption bands around 1800 cm^{-1} . Based on this fact and on the slow formation kinetics indicating an activated process, the species responsible for the band at 1620 cm^{-1} is rather assigned to a strongly bound NO derived surface species than to a typical nitrosyl. The exact nature of this entity is not clear yet. A comparison with previous work on NO/alumina at ambient pressures reveals, however, that absorption bands in this region are frequently observed and are typically assigned to surface nitrates, nitro or nitrito species [23,27,28]. The slow formation kinetics and the loss of the diffraction pattern is compatible with a restructuring process associated. Preferential sites at which this reaction might be initiated are defects sites on the oxide film, specifically oxide antiphase domain boundaries. The reason for the enhanced reactivity of these defects could arise from their modified electronic structure, which may facilitate an oxidation

processes [29]. Finally, it should be pointed out that a contribution of NO interacting with a Ni species from the NiAl support cannot be rigorously excluded on the basis of the present data. Based on a comparison with spectroscopic data for NO on oxygen precovered Ni [30] and NiO [21] surfaces this explanation appears rather unlikely, however. Moreover, it has recently been shown that the oxide antiphase domain boundaries are characterized by an inserted row of oxygen ions [29], and there are no indications that this structure facilitates diffusion of Ni to the surface.

The band (2) at 1690 cm^{-1} is due to an entity, which is formed only after substantial surface reconstruction. Similar to the band at 1620 cm^{-1} , it is assigned to a strongly bound NO derived surface species. Feature (2) is followed by an emerging high frequency band (1) at 1880 cm^{-1} . Absorption signals in this range have previously been assigned to the formation of NO dimers [17,18,20]. On oxidized Mo, formation of asymmetric dimers was observed, giving rise to two bands at 1871 and 1728 cm^{-1} [13]. The higher frequency band was assigned to a molecular vibration mainly localized at the outermost NO, whereas the more strongly bound inner NO gives rise to the low frequency feature. Analogous, we tentatively attribute band (1) at 1880 cm^{-1} to a NO species adsorbed on an NO derived entity (1690 cm^{-1}) on the strongly restructured Al_2O_3 film.

Dimer formation has been identified as an important pathway for NO decomposition at low temperature. On many surfaces, the NO dimer has been shown to decompose to N_2O and oxygen [16,18–20] and it is noteworthy that this reaction can occur at temperatures below 90 K [18]. Recently, conversion of NO to N_2O at 120 K was observed on MgO thin films and was suggested to occur at oxygen defects via NO dimer formation [31].

In experiments on Cu [18] and Ag [20] surfaces at sufficiently low temperature, adsorbed N_2O formed by NO decomposition, can be identified via two characteristic bands in the regions of 1250 – 1320 and 2230 – 2270 cm^{-1} . Thus, the bands (4) and (5) appearing in the low frequency region at 1304 and 1260 cm^{-1} may contain a contribution from adsorbed N_2O . The lack of bands in the high frequency region, however, suggests rapid

desorption of N_2O at 100 K [20]. An alternative explanation for the missing high frequency band would be a specific molecular orientation, leading to a vanishing IR activity due to the metal surface selection rule (MSSR) [32]. In any case it has to be taken into account that NO decomposition results in the accumulation of surface oxygen. In the presence of reactive oxygen species, produced via this process, further NO conversion to higher oxidized species is facilitated. Many of such species have been observed on alumina powders at higher pressure, such as e.g. linear, bridging and chelating nitro and nitrito species, different types of bridging and chelating nitrates as well as hyponitrites [23,24,26–28], although their exact identification remains controversial in many cases. Typically,

these species give rise to a variety of bands between 1000 and 1600 cm^{-1} . Based on their late appearance, features (4) and (5) and possibly also the broadening of band (1) may thus be tentatively attributed to such oxo-surface compounds of nitrogen.

In the second part of this work we investigate the interaction of NO with the alumina film after the growth of Pd particles (Fig. 3). As compared to the pristine film, a completely different behavior is observed. Whereas at an initial NO exposure of 11×10^{15} molecules cm^{-2} no absorption signals are observed on the pristine film, the spectrum of the Pd covered system has already reached its full absorption level. Three principal absorption regions are identified with bands at 1750 cm^{-1} (B), 1620 cm^{-1} (D) and 1542 cm^{-1} (E). The absorption

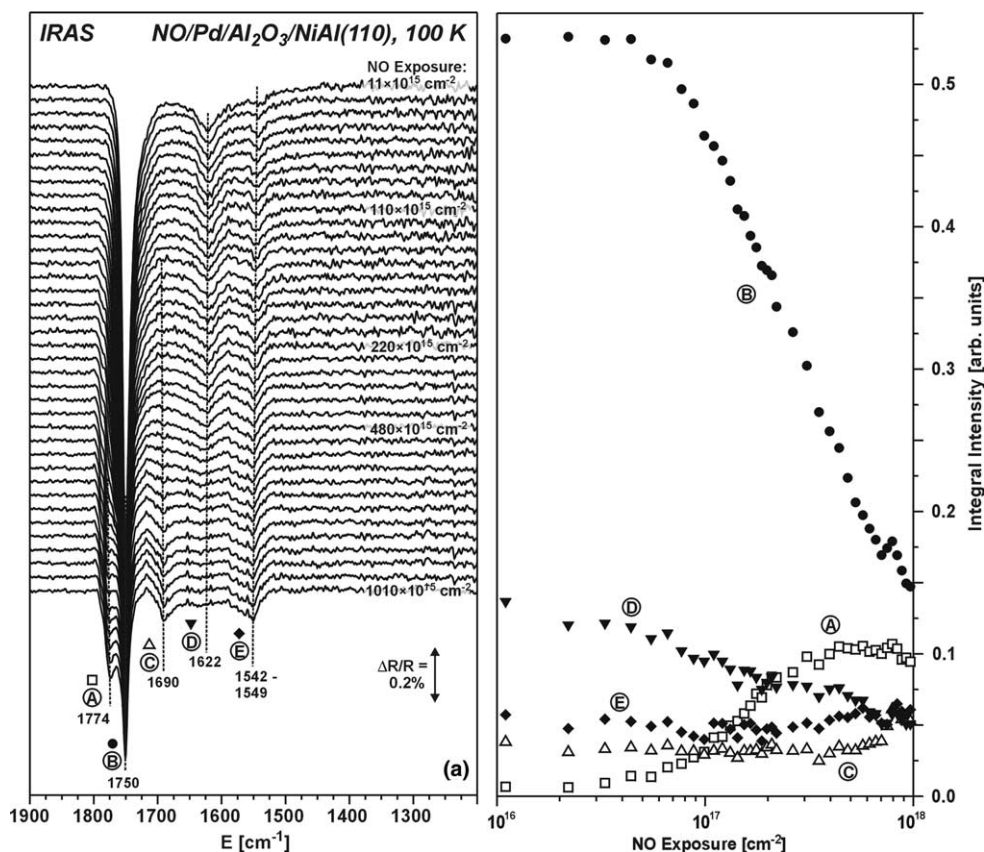


Fig. 3. (a) IR spectra acquired during exposure of the Al_2O_3 film on $\text{NiAl}(1\ 1\ 0)$ partially covered by Pd particles to a molecular beam of NO at a sample temperature of 100 K; (b) integral absorption of the different IR bands indicated in (a) as a function of NO exposure.

features are subject to a slow change affecting mainly the dominating band at 1750 cm^{-1} , which develops a high frequency shoulder at 1774 cm^{-1} (A). Finally, a weak feature at 1690 cm^{-1} in region (C) appears.

The rapid saturation of the NO bands on Pd is expected for chemisorption on the metal surface, which in contrast to nitrogen–oxygen-compound formation on alumina proceeds with a high sticking coefficient and without an appreciable activation barrier. Thus, we can immediately attribute all bands observed at low coverage to molecular NO on the Pd particles. A detailed assignment of most spectral features is possible on the basis of Pd single crystal data ([6] and references therein).

Briefly, we can assign the peak around 1750 cm^{-1} (B) to NO adsorbed in on-top geometry on Pd(111) facets and at particle defect sites, the band around 1620 cm^{-1} (D) to NO predominately at Pd edge, defect and (100) sites, and the feature around 1550 cm^{-1} (E) to NO on hollow sites, mainly on Pd(111). Note that the relative intensities of the bands do not reflect the relative concentrations of the corresponding species. This is a consequence of differences in the dynamic dipole moment, different molecular orientation and dipole coupling effects [33].

For the slow decrease of band (B) and the simultaneous appearance of the high frequency shoulder (A) there are two possible explanations:

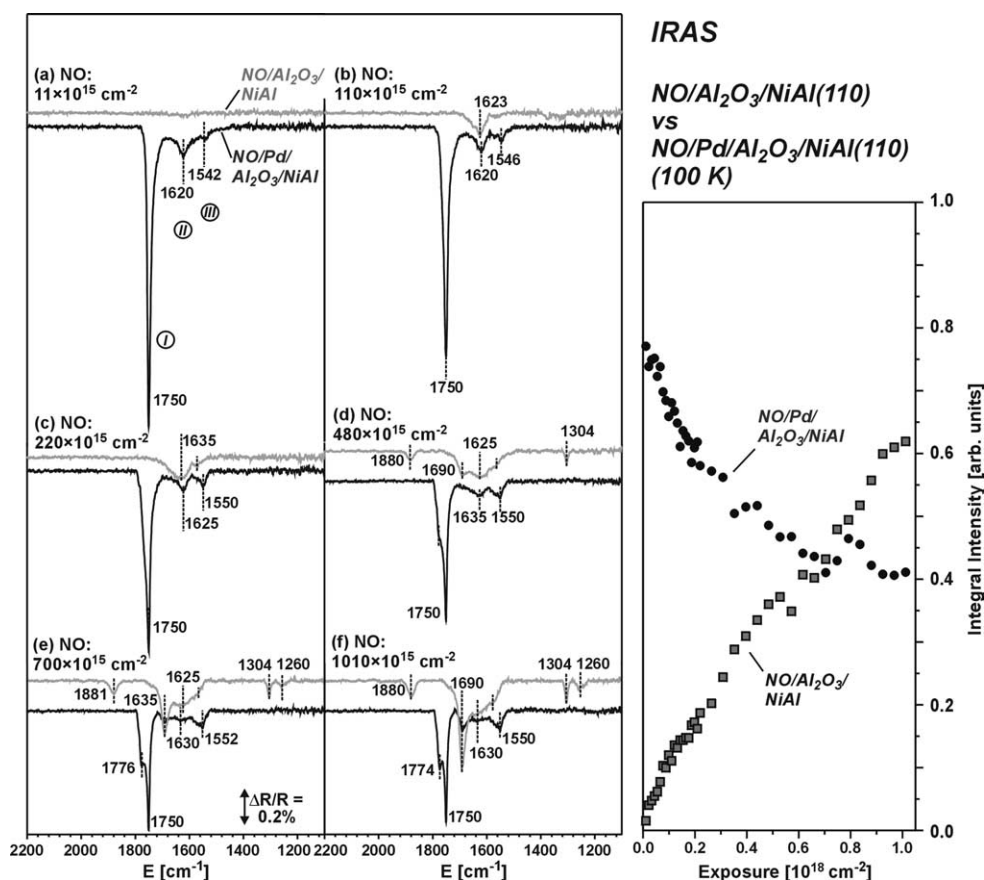


Fig. 4. Comparison of IR spectra of the pristine Al_2O_3 film (gray traces) and the Al_2O_3 film partially covered by Pd particles (black traces) at different NO exposures (left). Total integral absorption in the NO stretching frequency region as a function of NO exposure (right).

First, the shoulder may be due to the presence of surface contaminations. A possible candidate would be co-adsorbed oxygen, which e.g. might be produced via NO decomposition on the support. This appears unlikely, however, as the shoulder emerges well before first indications for a support interaction are observed. Moreover, oxygen co-adsorption studies show strong blue-shifts not only for the on-top band but for other NO absorption features as well [6]. An alternative explanation involves the formation of a high coverage adsorbate structure, which due to a low adsorbate mobility and a low sticking coefficient may develop only slowly and at high NO doses.

Comparing the spectra of the Pd covered and Pd free support, the most surprising observation is the absence of several bands (1880, 1304 and 1260 cm^{-1}) which are characteristic for the NO decomposition process. This becomes particularly evident, if we directly compare the IR spectra for the pristine and Pd covered alumina film at identical NO exposures (Fig. 4a). Only at highest NO doses, a weak feature at 1690 cm^{-1} (C) appears, which coincides with the band (2) observed on the pristine alumina film and may be indicative for a minor amount of a nitrogen–oxygen compound being formed. A comparison of the total integral intensities in the NO region is displayed in Fig. 4b. Whereas for the pristine oxide film the total absorption increases nearly linearly up to high NO exposures, immediate saturation occurs in the case of the partially Pd covered oxide (the following decrease is mainly due to the slow transformation to the high coverage structure; see above).

This observation suggests that the low temperature NO decomposition processes are strongly inhibited on the Pd covered oxide film. Based on the growth behavior of the Pd particles, we propose as a possible explanation that the restructuring and redox processes involving NO require specific defect sites to be initiated. The antiphase domain boundaries may provide a geometric and electronic structure, which could facilitate this reaction. With the Pd particles efficiently covering these defects, they also prevent the initial step of the decomposition sequence, leading to the observed inertness of the oxide after metal deposition. It is likely that the restructuring process is

facilitated by an enhanced interaction of NO with the oxide defect structure and/or by specific structural and redox properties of these sites.

In conclusion, we have studied the interaction and decomposition of NO on a well-ordered Al_2O_3 film, before and after growth of Pd crystallites. On the pristine Al_2O_3 film, NO undergoes a slow decomposition process at 100 K. The process is initiated at oxide defects and involves a strong structural transformation of the oxide. Different types of nitrogen–oxygen derived species are successively formed, including the formation and decomposition of NO dimers. After growth of the Pd particles on $\text{Al}_2\text{O}_3/\text{NiAl}(1\ 1\ 0)$, the decomposition pathway observed on the pristine film is strongly inhibited. Instead, NO adsorption is observed to occur on the Pd particles only. It is concluded that the decomposition pathway is initiated at specific oxide defect sites, which are efficiently covered by the metal.

Acknowledgements

Financial support of this project by the Volkswagen Foundation is acknowledged. We are grateful to Dr. C.S. Gopinath for helpful discussions.

References

- [1] T. Kreuzer, S.E. Lox, D. Lindner, J. Leyrer, *Catal. Today* 29 (1996) 17.
- [2] M. Bäumer, H.-J. Freund, *Prog. Surf. Sci.* 61 (1999) 127.
- [3] I. Meusel, J. Hoffmann, J. Hartmann, M. Heemeier, M. Bäumer, J. Libuda, H.-J. Freund, *Catal. Lett.* 71 (2001) 5.
- [4] S. Shaikhutdinov, M. Heemeier, J. Hoffmann, I. Meusel, B. Richter, M. Bäumer, H. Kuhlenbeck, J. Libuda, H.-J. Freund, R. Oldman, S.D. Jackson, C. Konvicka, M. Schmid, P. Varga, *Surf. Sci.* 501 (2002) 270.
- [5] J. Libuda, H.-J. Freund, *J. Phys. Chem. B* 106 (2002) 4901.
- [6] S. Schauer mann, V. Johánek, J. Hoffmann, M. Laurin, J. Libuda, H.-J. Freund, *Phys. Chem. Chem. Phys.*, in press.
- [7] V. Johánek, S. Schauer mann, M. Laurin, J. Libuda, H.-J. Freund, *Angew. Chem. Int. Ed.* 42 (2003) 3035.
- [8] V. Johánek, S. Schauer mann, M. Laurin, C.S. Gopinath, J. Libuda, H.-J. Freund, submitted.
- [9] J. Libuda, I. Meusel, J. Hartmann, H.-J. Freund, *Rev. Sci. Instrum.* 71 (2000) 4395.

- [10] J. Libuda, F. Winkelmann, M. Bäumer, H.-J. Freund, T. Bertrams, H. Neddermeyer, K. Müller, *Surf. Sci.* 318 (1994) 61.
- [11] M. Frank, M. Bäumer, *Phys. Chem. Chem. Phys.* 2 (2000) 3723.
- [12] R.M. Jaeger, Ph.D. Thesis, Bochum, 1992.
- [13] K.T. Queeney, S. Pang, C.M. Friend, *J. Chem. Phys.* 109 (1998) 8058.
- [14] K.T. Queeney, C.M. Friend, *Surf. Sci.* 414 (1998) L957.
- [15] K.T. Queeney, C.M. Friend, *J. Phys. Chem. B* 102 (1998) 9251.
- [16] K.T. Queeney, C.M. Friend, *J. Chem. Phys.* 107 (1997) 6432.
- [17] W.A. Brown, P. Gardner, M.P. Jigato, D.A. King, *J. Chem. Phys.* 102 (1995) 7277.
- [18] W.A. Brown, P. Gardner, D.A. King, *J. Phys. Chem.* 99 (1995) 7065.
- [19] P. Dumas, M. Suhren, Y.J. Chabal, C.J. Hirschmugl, G.P. Williams, *Surf. Sci.* 371 (1997) 200.
- [20] W.A. Brown, R.K. Sharma, D.A. King, *J. Phys. Chem.* 100 (1996) 12559.
- [21] M. Schönnenbeck, D. Cappus, J. Klinkmann, H.-J. Freund, L.G.M. Pettersson, P.S. Bagus, *Surf. Sci.* 347 (1996) 337.
- [22] M. Wilde, O. Seiferth, K. Al-Shamery, H.-J. Freund, *J. Chem. Phys.* 111 (1999) 1158.
- [23] T. Venkov, K. Hadjiivanov, D. Klissurski, *Phys. Chem. Chem. Phys.* 4 (2002) 2443.
- [24] T.E. Hoost, K. Otto, K.A. Laframboise, *J. Catal.* 155 (1995) 303.
- [25] D.K. Paul, B.W. Smith, C.D. Marten, J. Burchett, *J. Mol. Catal. A* 167 (2001) 67.
- [26] B. Westerberg, E. Fridell, *J. Mol. Catal. A* 165 (2001) 249.
- [27] C. Sedlmair, K. Seshan, A. Jentys, J.A. Lercher, *J. Catal.* 214 (2003) 308.
- [28] K.I. Hadjiivanov, *Catal. Rev. Sci. Eng.* 42 (2000) 71.
- [29] M. Kulawik, N. Nilius, H.-P. Rust, H.-J. Freund (submitted).
- [30] J.G. Chen, W. Erley, H. Ibach, *Vacuum* 41 (1990) 74.
- [31] C.D. Valentin, G. Pacchioni, S. Abbet, U. Heiz, *J. Phys. Chem. B* 106 (2002) 7666.
- [32] F.M. Hoffmann, *Surf. Sci. Rep.* 3 (1983) 107.
- [33] P. Hollins, *Surf. Sci. Rep.* 16 (1992) 51.